HAL
open science

Hydrogen bonding interactions in single component molecular conductors based on metal (Ni, Au) bis(dithiolene) complexes

Hadi Hachem, Nathalie Bellec, Marc Fourmigué, Dominique Lorcy

To cite this version:

Hadi Hachem, Nathalie Bellec, Marc Fourmigué, Dominique Lorcy. Hydrogen bonding interactions in single component molecular conductors based on metal (Ni, Au) bis(dithiolene) complexes. Dalton Transactions, 2020, 40 (18), pp.6056-6064. 10.1039/d0dt00960a . hal-02563403

HAL Id: hal-02563403

https://univ-rennes.hal.science/hal-02563403

Submitted on 11 Jun 2020

HAL is a multi-disciplinary open access archive for the deposit and dissemination of scientific research documents, whether they are published or not. The documents may come from teaching and research institutions in France or abroad, or from public or private research centers.

L'archive ouverte pluridisciplinaire **HAL**, est destinée au dépôt et à la diffusion de documents scientifiques de niveau recherche, publiés ou non, émanant des établissements d'enseignement et de recherche français ou étrangers, des laboratoires publics ou privés.

View Article Online
DOI: 10.1039/D0DT00960A

Hydrogen bonding interactions in single component molecular conductors based on metal (Ni, Au) bis(dithiolene) complexes†

Hadi Hachem, Nathalie Bellec, Marc Fourmigué* and Dominique Lorcy*

Univ Rennes, CNRS, ISCR (Institut des Sciences Chimiques de Rennes) - UMR 6226, F-35000 Rennes, France. Email : marc.fourmigue@univ-rennes1.fr, dominique.lorcy@univ-rennes1.fr

D. Lorcy https://orcid.org/0000-0002-7698-8452
M. Fourmigué https://orcid.org/0000-0002-3796-4802

† Electronic supplementary information (ESI) available: Figs S1-S5 and details on band structure calculations. X-ray data are available in CIF format. CCDC 1989996−1989998. For ESI and crystallographic data in CIF format see DOI: 10.1039/XXXXX

Abstract

Introduction of hydrogen bonding (HB) interactions in single component conductors derived from nickel and gold bis(dithiolene) complexes is explored with the 2-alkylthio-1,3-thiazole-4,5-dithiolate (RS-tzdt) with R = CH_2CH_2OH through the preparation of the neutral $[Ni(HOEtS\text{-}tzdt)_2]^0$ (closed-shell) and $[Au(HOEtS\text{-}tzdt)_2]^{\bullet}$ (radical) complexes. At variance with many other radical gold dithiolene complexes which have a strong tendency to dimerize in the solid state, $[Au(HOEtS\text{-}tzdt)_2]^{\bullet}$ crystallizes into uniform stacks interconnected by strong O−H•••N HB involving the nitrogen atom of the thiazole ring. $[Au(HOEtS\text{-}tzdt)_2]^{\bullet}$ is isostructural with its neutral, closed-shell nickel analog $[Ni(HOEtS\text{-}tzdt)_2]^0$, a rare situation in this metal bis(dithiolene) chemistry. It demonstrates how the strength of the HB directing motif can control the overall structural arrangement to stabilize the same structure despite a different electron count. The nickel complex behaves as a band semiconductor with weak room temperature conductivity (1.6×10^{-5} S.cm^{-1}), while the gold complex is described as a Mott insulator with a three orders of magnitude improved conductivity (6×10^{-2} S.cm^{-1}).

Published on 08 April 2020. Downloaded by Bibliotheque de L'Universite de Rennes I on 4/8/2020 12:41:09 PM.

Accepted manuscript

Manuscipt

View Article Online
DOI: 10.1039/D0DT00960A

Published on 08 April 2020. Downloaded by Bibliotheque de L'Universite de Rennes I on 4/8/2020 12:41:09 PM.

Introduction

Intermolecular interactions and packing of electroactive molecules such as metal bis(dithiolene) complexes play a critical role in the conducting properties of these molecular materials.[1] Most of these conducting materials involve open shell species, either charged ones, as in the various nickel bis(dithiolene) complexes involving radical anion species such as $[Ni(dmit)_2]^{1-}$,[2,3,4,5,6,7,8,9,10,11] or neutral radical species such as gold bis(dithiolene) complexes.[12,13,14,15,16,17] Essentially all reported examples of such conducting systems are based on dithiolene ligands deprived of any functional groups known to induce other specific intermolecular interactions than the recurrent overlap of sulfur-rich moieties, starting with the strongest of them, hydrogen bonding. Indeed, to our knowledge, only a handful of examples have been reported (Chart 1) where the dithiolene ligand itself is functionalized with for example an amide,[18,19,20] an imide,[18] a primary alcohol,[21,22] or a catechol moiety.[23] This is all the more surprising when one considers the numerous examples reported in the chemistry of *cation* radical salts derived from tetrathiafulvalene derivatives bearing such HB donor groups.[24]

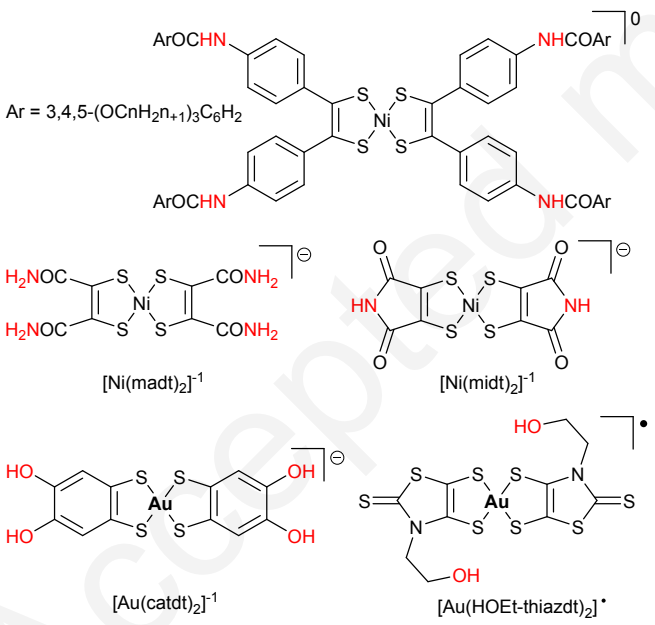

Chart 1 Reported dithiolene complexes with hydrogen bond donor groups.

Among functionalized bis(dithiolene) complexes, we recently reported complexes built out of the electron rich *N*-alkyl-1,3-thiazoline-2-thione-4,5-dithiolate (R-thiazdt) ligand,[25] and particularly the one with an 2-hydroxyethyl substituent, R = CH_2CH_2OH (Chart 1).[22] The neutral radical complex, $[Au(HOEt\text{-}thiazdt)_2]^{\bullet}$, was shown to organize into regular stacks as its ethyl analogue, $[Au(Et\text{-}thiazdt)_2]^{\bullet}$.[26] It behaves as a semiconductor ($\sigma_{RT} = 5{-}7\times10^{-2}$ S cm^{-1}) at

Accepted manuscript
Manuscipt

View Article Online
DOI: 10.1039/D0DT00960A

room temperature and ambient pressure with an activation energy of 0.14 eV. Comparison of the crystal structures and transport and magnetic properties with those of the reference [Au(Et-thiazdt)$_2$]$^{\bullet}$ single-component conductor[26] showed that the replacement of ethyl by the slightly bulkier hydroxyethyl substituent affected only weakly the overlap interactions, while introducing lateral O−H•••S hydrogen bonding interactions with the outer C=S moiety.

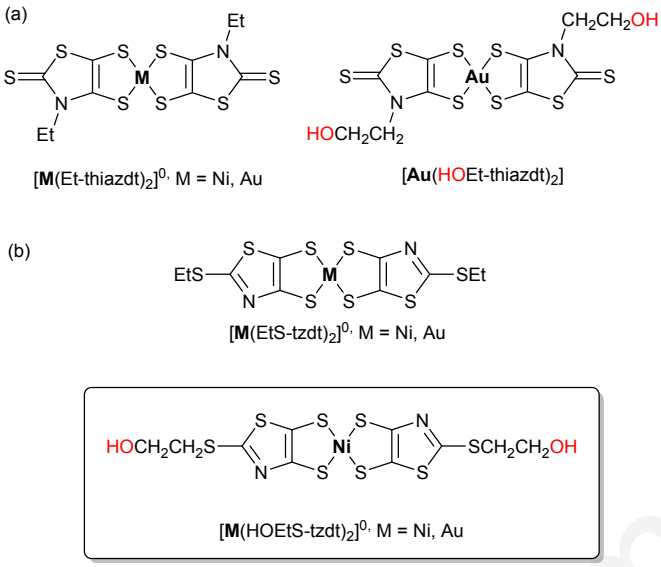

Chart 2 [M(R-thiazdt)$_2$] *vs.* [M(RS-tzdt)$_2$] complexes, M = Ni, Au.

Such radical gold complexes also allow for the formation of single component molecular conductors.[26,27,28,29,30,31] Besides these open-shell gold complexes, only a few studies report on the conducting properties of single component molecular conductors based on formally *closed-shell* nickel bis(dithiolene) complexes. We can mention here the highly conducting neutral nickel bis(dithiolene) complexes bearing a non-innocent tetrathiafulvalene (TTF) backbone.[32,33,34,35,36,37] Without this TTFdithiolate backbone, only few examples of Ni complexes lead to conducting materials with room temperature conductivity higher than 10^{-5} S.cm^{-1}. For instance, the neutral closed-shell [Ni(dmit)$_2$]^0 (dmit: 4,5-dimercapto-1,3-dithiole-2-thione) complex behaves as a single component molecular conductor (σ_{RT} = 3.5×10^{-3} S.cm^{-1})[38] which turns even metallic under very high pressures (above 15.9 GPa).[39] Within this frame we demonstrated that [Ni(Et-thiazdt)$_2$]^0 (Chart 2a), with this electron rich *N*-ethyl-1,3-thiazoline-2-thione-4,5-dithiolate (Et-thiazdt) ligand, could also behave as a single component molecular conductor ($\sigma_{RT} \approx 1.4\times10^{-2}$ S cm^{-1}).[40] Due to its closed-shell character, this neutral nickel complex behaves as classical band semiconductor while its gold analogue, the open-shell [Au(Et-thiazdt)$_2$]$^{\bullet}$, behaves as a Mott insulator.[26] We also recently investigated another ligand,

Published on 08 April 2020. Downloaded by Bibliotheque de L'Universite de Rennes I on 4/8/2020 12:41:09 PM.

Accepted Manuscript

Manuscipt

View Article Online
DOI: 10.1039/D0DT00960A

Published on 08 April 2020. Downloaded by Bibliotheque de L'Universite de Rennes I on 4/8/2020 12:41:09 PM.

isomer to the R-thiazdt ligand, the 2-alkylthio-1,3-thiazole-4,5-dithiolate (RS-tzdt) (Chart 2b). With R = Et, we compared the overlap interactions between the corresponding neutral gold (radical) and nickel (closed-shell) complexes, namely $[Au(EtS\text{-}tzdt)_2]^{\bullet}$,[41] and $[Ni(EtS\text{-}tzdt)_2]^0$.[42] A strong difference was found between these Ni and Au complexes as the $[Ni(EtS\text{-}tzdt)_2]^0$ complex forms uniform stacks in the solid state while for the gold complex, $[Au(EtS\text{-}tzdt)_2]^{\bullet}$, dimerization occurs.

With these results in mind, we decided to introduce the 2-hydroxyethyl HB donor group within this novel family of dithiolene ligands, the 2-alkylthio-1,3-thiazole-4,5-dithiolate (RS-tzdt), with R = CH_2CH_2OH, with the aim to unravel the role of HB in the structural and electronic properties of both the Ni and Au complexes. Herein, we report the synthesis of the neutral Ni (closed-shell) and Au (radical) complexes formulated as $[Ni(HOEtS\text{-}tzdt)_2]^0$ and $[Au(HOEtS\text{-}tzdt)_2]^{\bullet}$. We investigate their solid state structural and electronic properties, highlighting the role of the intermolecular hydrogen bonding interactions in the outcome of their competition/synergy with the overlap interactions between the radical complexes when M = Au at variance with the closed-shell Ni complex.

Results and discussion

Syntheses and spectroscopic properties of monoanionic complexes.

The neutral complexes were obtained by electrocrystallization of the corresponding monoanionic Ni and Au complexes. The latter are prepared starting from the N-*t*Bu-1,3-thiazoline-2-thione proligand **1** as outlined in Scheme 1. The synthesis of 2-(hydroxyethylthio)-1,3-thiazole-4,5-dithiolene proligand **2** involves the reaction of **1** in the presence of an excess of 2-iodoethanol. This original transformation, first discovered with simple alkylating reagents such as MeI or EtI,[42] has been successfully extended here to 2-iodoethanol. When the reaction was performed in refluxing dichloromethane, as previously described with MeI and EtI, the proligand **2** was obtained in very low yield (7%) only. This disappointing result was circumvented by using a more polar solvent such as DMF and extending the reaction time. After 16h at 80°C in the presence of an excess of 2-iodoethanol, we isolated **2** in 68 % yield. Deprotection of the proligand **2** in the presence of sodium methanolate, followed by the addition of $NiCl_2.6H_2O$ or $KAuCl_4$ and PPh_4Br leads to the formation of the monoanionic complexes as tetraphenylphosphonium salts, $[PPh_4][Ni(HOEtS\text{-}tzdt)_2]$ and $[PPh_4][Au(HOEtS\text{-}tzdt)_2]$, recrystallized from CH_2Cl_2/MeOH and CH_3CN respectively. Only the gold complex $[PPh_4][Au(HOEtS\text{-}tzdt)_2]$ afforded crystals amenable to X-ray diffraction.

Accepted manuscript

Manuscipt

View Article Online
DOI: 10.1039/D0DT00960A

Published on 08 April 2020. Downloaded by Bibliotheque de L'Universite de Rennes I on 4/8/2020 12:41:09 PM.

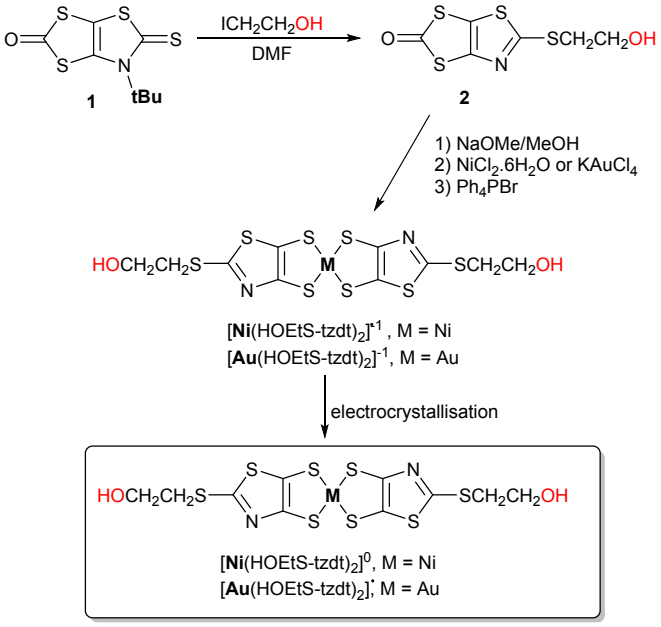

Scheme 1 Synthetic route towards the neutral nickel and gold complexes [M(HOEtS-tzdt)$_2$], (M = Ni, Au).

The crystal structure of [PPh$_4$][Au(HOEtS-tzdt)$_2$] is solved in the monoclinic system, space group P2$_1$/c. The unit cell contains three crystallographically independent gold complexes and three PPh$_4^+$ cations, all in general position. The three complexes have a similar geometry, with a planar structure and a *trans* configuration of the ligands (Fig. 1). The Ph$_4$P$^+$ organize as "parallel quadruple phenyl embrace motif" (Fig. S1) similar to what was seen for the [PPh$_4$][Ni(EtS-tzdt)$_2$].[42] A complex set of hydrogen bonds (Fig. 1) takes place in the crystal, whose structural characteristics are collected in Table 1. They point toward strong and directional HB interactions,[43,44] which involve not only the hydroxyl oxygen atoms as HB acceptors but also the sp$_2$ nitrogen atom of the thiazole ring, a specificity of this tzdt ligand.

Accepted manuscript

Manuscipt

View Article Online
DOI: 10.1039/D0DT00960A

Published on 08 April 2020. Downloaded by Bibliotheque de L'Universite de Rennes I on 4/8/2020 12:41:09 PM.

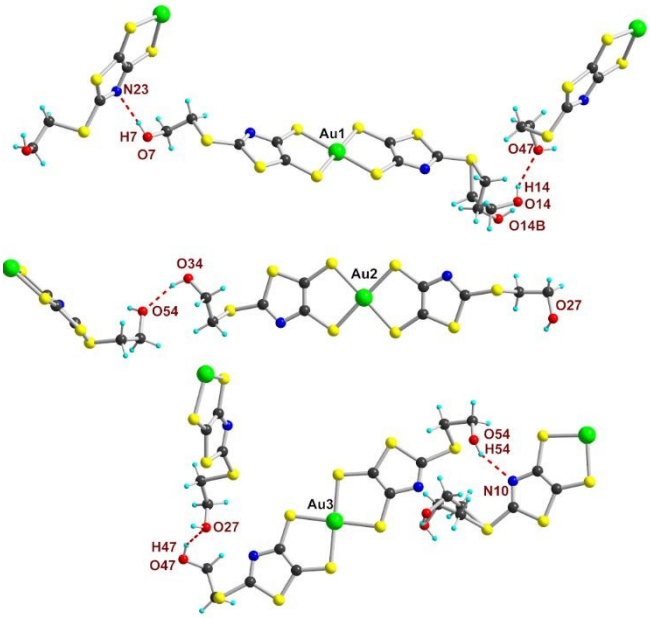

Fig. 1 Detail of the three crystallographically independent anions in $[PPh_4][Au(HOEtS\text{-}tzdt)_2]$ with the hydrogen bonding interactions their hydroxyl groups develop with neighboring molecules (red dotted lines).

Table 1 Structural characteristics of hydrogen bonds in $[PPh_4][Au(HOEtS\text{-}tzdt)_2]$. The reduction ratio (RR) is defined as the actual H•••O(N) distance divided by the van der Waals contact distance (H•••O: 2.72 Å; H•••N: 2.75 Å)

	Distances (Å)	RR	Angles (°)
O7−H7•••N23	2.123(7))	0.77	166.3(7)
O14−H14•••O47	2.165(15)	0.80	129.3(1))
O27−H27	–	–	–
O34−H34•••O54	1.976(16)	0.73	162.3(9)
O47−H47•••O27	2.019(16)	0.75	147.6(9)
O54−H54•••N10	2.161(9)	0.78	137.2(9)

The redox properties of the two complexes $[PPh_4][M(HOEtS\text{-}thiazdt)_2]$ (M = Ni, Au) were determined by cyclic voltammetry (CV) and the redox potentials are collected in Table 2 together with those of the ethyl derivative, $[PPh_4][M(EtS\text{-}thiazdt)_2]$, for comparison. The CVs of the nickel complex (Fig. S2) presents one well defined redox process corresponding to the oxidation of the dianionic complex into the monoanion radical, if the scan is performed between −0.7 V and −0.2 V vs SCE. On the other hand, upon scanning to more anodic potentials, a second pseudo-reversible process is observed, corresponding to the oxidation of the monoanion

Accepted Manuscript

View Article Online
DOI: 10.1039/D0DT00960A

Published on 08 April 2020. Downloaded by Bibliotheque de L'Universite de Rennes I on 4/8/2020 12:41:09 PM.

into the neutral complex, followed on the reverse scan by a modification of the first reduction process with the appearance of a sharp desorption reduction peak due to the adsorption of an oxidized species on the electrode. As previously observed for other Ni complexes with the same family of ligand, the first redox process occurs at a low oxidation potential at the origin of the isolation of the monoanionic species under air atmosphere following the initial preparation of the dianionic species. For the gold complex $[PPh_4][Au(HOEtS\text{-}thiazdt)_2]$, on the anodic scan (Fig. S2), only one redox process is observed corresponding to the oxidation of the monoanion into the neutral radical species while on the cathodic scan an irreversible reduction process is detected corresponding to the reduction of the monoanion into the dianionic Au(II) species.[45] Interestingly in both cases, the replacement of the ethyl substituent by the 2-hydroxyethyl one induces, for the oxidation of the monoanionic species into the neutral one, a shift of about 40-50 mV towards less anodic potentials, as well as a loss of reversibility, due to the electrodeposition of the neutral species at the electrode.

.

Table 2 Redox potentials (E in V *vs*. SCE) determined in CH_2Cl_2 with 0.1M NBu_4PF_6, at 100 $mV.s^{-1}$ and Wavelength (nm) of the absorption maxima, and the respective molar extinction coefficients ($M^{-1}.cm^{-1}$) of the monoanions in the UV-Vis-NIR region.

	E_{pa}/E_{pc} (−2/−1)	E_{pa}/E_{pc} (−1 /0)	$\lambda_{max}(\varepsilon)$	Ref.
$[PPh_4][Ni(HOEtS\text{-}tzdt)_2]$	−0.43/−0.48	+0.14/−0.02	1064, (15 300)	this work
$[PPh_4][Ni(EtS\text{-}tzdt)_2]$	−0.43/−0.50	+0.19/+0.12	1076 (13 200)	42
$[PPh_4][Au(HOEtS\text{-}tzdt)_2]$	−1.12	+0.45/+0.28	366 (14 200) 294 (30 700)	this work
$[PPh_4][Au(EtS\text{-}tzdt)_2]$	−1.04	+0.48/+0.44	360(13 000) 296(18 700)	42

The UV-Vis-NIR spectroscopic investigations of the monoanionic complexes were carried out in dichloromethane solution ($C = 10^{-5}$ M) at room temperature (Fig. S3). The values of the absorption maxima and their extinction coefficients for the studied gold and nickel complexes are collected in Table 2. The nickel monoanionic complexes exhibit low energy band absorptions in the NIR region that are attributed to π–π^* transitions while the monoanionic gold complexes show absorptions that are limited to the UV-Vis region. This result is not surprising given the fact that the monoanionic gold complexes are isoelectronic to the dianionic nickel complexes, with no low energy transitions. The observed absorptions for $[Ni(RS\text{-}tzdt)_2]^{-1}$ are in the range of 1064-1076 nm, which is notably blue shifted compared to the N-

Accepted Manuscript

View Article Online
DOI: 10.1039/D0DT00960A

substituted thiazoline-2-thione complexes that absorb in the 1228-1280 nm range. A possible explanation for this shift, is that the aromaticity of the thiazole ring confines the π electrons on the aromatic ring, limiting the extent of the delocalization, which is a well-known phenomenon in conducting polymers.[46]

Published on 08 April 2020. Downloaded by Bibliotheque de L'Universite de Rennes I on 4/8/2020 12:41:09 PM.

Syntheses and spectroscopic properties of neutral complexes.

The neutral complexes were generated through electrocrystallization of the monoanionic species. Upon application of a constant current of 0.2 μA to a solution of the monoanionic complex in CH_2Cl_2/CH_3CN containing Bu_4NPF_6 as supporting electrolyte, crystals of the two neutral complexes were collected at the anode after seven days. X-ray diffraction analyses show that the complexes [M(HOEtS-tzdt)$_2$] (M = Ni, Au), are isostructural, and crystallize in the monoclinic system, space group P2$_1$/n with the metal complex located on inversion center, with the *trans* configuration and a planar skeleton. Actually, upon oxidation a planarization of the metallacycles occurs as the dihedral angles along the S•••S hinge amount to 0.49-7.24° in the monoanions and 0.23° in the neutral complex. The hydroxyethyl chains are not located in the molecular plane as observed for the ethyl analogues [M(EtS-tzdt)$_2$] (M = Au,[41] Ni),[42] but point out of this plane.

In the solid state, the complexes form uniform stacks along *a* interacting sideways within (ac) layers (Figure 2). The plane-to-plane distance between the neighboring molecules amounts to 3.61 Å and 3.63 Å for the nicked and the gold complexes respectively. Hydrogen bonding interactions develop between the complexes belonging to neighboring stacks along the *c* direction and involve the OH group as HB donor and the nitrogen of the thiazole ring as HB acceptor (Fig. 2, Fig. S4). The O−H•••N distances amount to 1.968 Å, and 2.065 Å for the nickel and gold complexes respectively, corresponding to 0.71 and 0.75 reduction ratio relative to the sum of the vdW radii of nitrogen and hydrogen (2.75 Å). They are notably shorter than those observed in the anionic gold complex [Au(HOEtS-tzdt)^2]$^{1-}$ (See Table 1). The O−H•••N angles are 168.8°, and 158.2° for the nickel and gold complex respectively, indicating also a high degree of directionality of this noncovalent interaction.

Accepted Manuscript

Manuscipt

View Article Online
DOI: 10.1039/D0DT00960A

Published on 08 April 2020. Downloaded by Bibliotheque de L'Universite de Rennes I on 4/8/2020 12:41:09 PM.

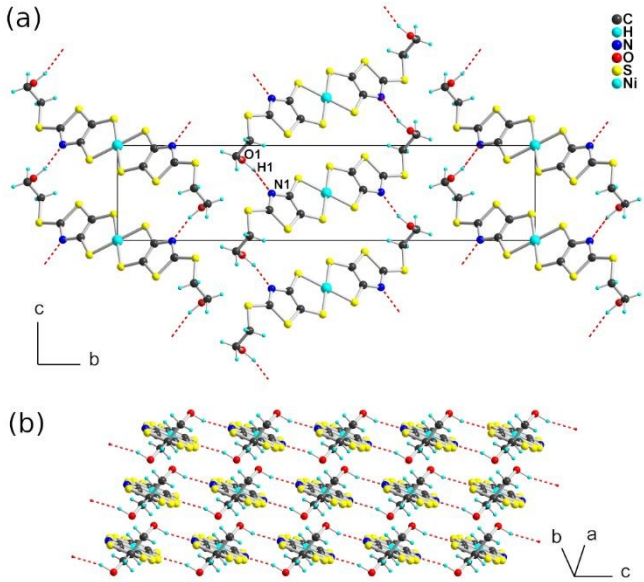

Fig. 2 Hydrogen-bonded chains of $[Ni(HOEtS\text{-}tzdt)_2]^0$ running along *c*. The gold complex $[Au(HOEtS\text{-}tzdt)_2]^{\bullet}$ is isostructural.

It is of interest to compare the molecular structures of these hydroxyethyl substituted complexes $[M(HOEtS\text{-}tzdt)_2]$ (M = Au, Ni) with the ones of their ethyl analogues $[M(EtS\text{-}tzdt)_2]$ (M = Au,[41] Ni)[42] in order to analyze the influence of the hydrogen bond on the overall organization of these complexes in the solid state. First of all, the ethyl analogues are neither isostructural with each other nor with the hydroxyethyl complexes (Table 3). The ethyl radical gold complexes $[Au(EtS\text{-}tzdt)_2]^{\bullet}$ are organized into dimers –a consequence of their open-shell character− while the nickel complexes $[Ni(EtS\text{-}tzdt)_2]^0$ formed regular stacks. Herein, both the closed-shell nickel complex and the open-shell gold complex $[M(HOEtS\text{-}tzdt)_2]$ (M = Au, Ni) form regular stacks. Another striking feature concerns the overlap pattern of these complexes (Figure 3). For the ethyl substituted open-shell gold complex, they form almost eclipsed dimers associated with the formation of a 2e− bonding interaction between radicals, while for the closed-shell nickel complex a pronounced lateral and longitudinal slip is observed, but different from what is found here for the hydroxyethyl complexes $[M(HOEtS\text{-}tzdt)_2]$ (M = Au, Ni). Interestingly the presence of the hydroxyethyl chain and its role for promoting strong HB interactions between stacks allows for the formation of uniform stacks, a prerequisite to observe higher conductivity in these single-component conductors. In other words, we can consider that the introduction of the strong O−H•••N HB avoided the radical dimerization.

Accepted manuscript

Manuscipt

View Article Online
DOI: 10.1039/D0DT00960A

Published on 08 April 2020. Downloaded by Bibliotheque de L'Universite de Rennes I on 4/8/2020 12:41:09 PM.

Table 3 Compared unit cell parameters of [M(HOEtS-tzdt)$_2$] and [M(EtS-tzdt)$_2$] (M = Au, Ni) neutral complexes

Complexes	[Ni(HOEtS-tzdt)$_2$][a]	[Au(HOEtS-tzdt)$_2$][a]	[Ni(EtS-tzdt)$_2$][b]	[Au(EtS-tzdt)$_2$][c]
System	monoclinic	monoclinic	triclinic	triclinic
Space group	P2$_1$/n	P2$_1$/n	$P\bar{1}$	$P\bar{1}$
a (Å)	5.0235(3)	4.9715(6)	6.6193(6)	7.5056(4)
b (Å)	27.1171(19)	27.272(3)	4.0075(4)	7.9184(4)
c (Å)	6.1914(4)	6.1720(8)	15.4038(14)	15.1842(8)

[a] This work. [b] Ref. 42. [c] Ref. 41

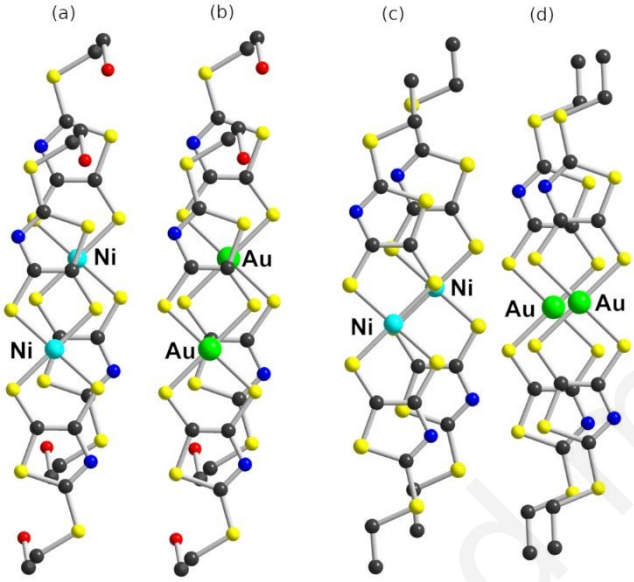

Fig. 3 Comparison of the overlap pattern of (a) [Ni(HOEtS-tzdt)$_2$]^0, (b) [Au(HOEtS-tzdt)$_2$]$^{\bullet}$, and the reported (c) [Ni(EtS-tzdt)$_2$]^0 and (d) [Au(EtS-tzdt)$_2$]$^{\bullet}$ complexes.

Despite the fact of being isostructural, the nickel and gold complexes [M(HOEtS-tzdt)$_2$] (M = Au, Ni), present a different electron count which should have an influence on their electronic properties. Indeed, the room temperature conductivity at ambient pressure, σ_{RT}(1 bar) amounts to 6×10^{-2} S.cm^{-1} for the gold complex and to 1.6×10^{-5} S.cm^{-1} for the nickel one, that is almost three orders of magnitude smaller with nickel. The gold complex exhibits a weak temperature independent paramagnetism (χ_0 = 0.56 10^{-4} cm^3.mol^{-1} at room temperature, Fig. S5) in accordance with a Pauli-type susceptibility of a good conductor. This χ_0 value is in the range with the one found for the gold complex [Au(Et-thiazdt)$_2$] ($\chi_0 = 10^{-4}$ cm^3.mol^{-1}) with a room temperature conductivity of 0.33 S. cm^{-1} behaving as a Mott insulator.[26] At lower temperatures, a Curie tail corresponding to 5.8 % S = ½ species is attributable to paramagnetic defaults. This difference in conductivity values between the two complexes, [M(HOEtS-tzdt)$_2$]

Accepted Manuscript

View Article Online
DOI: 10.1039/D0DT00960A

(M = Au, Ni) finds its rationale in their band structures which derive from the specific overlap interactions between molecules in the crystal.

The two isostructural complexes exhibit three types of overlap interactions within the *ac* plane depicted in Fig. 4. Their extent has been evaluated from the calculation of the $\beta_{HOMO-HOMO}$, $\beta_{HOMO-LUMO}$ and $\beta_{LUMO-LUMO}$ interaction energies for the Ni complex and the $\beta_{SOMO-SOMO}$ overlap interactions for the Au complex (Table 4). In both complexes, the strongest interactions are the ones within the stacks (Type I) while the second strongest ones (Type II) are established between complexes that are also linked by the O−H•••N hydrogen bonds (Cf. Fig. 2 and Fig. S4).

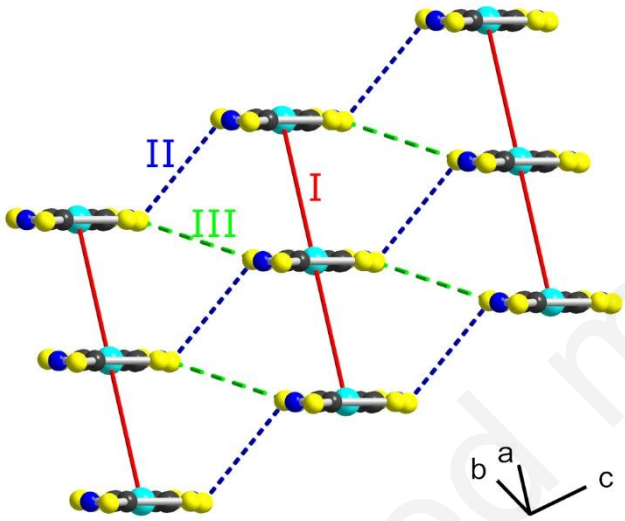

Fig. 4 Side view of the conducting slabs of [Ni(HOEtS-tzdt)$_2$] with intermolecular interactions. Notation for the Au complex is identical. The hydroxyethyl moieties have been omitted for clarity.

Table 4 Calculated β interaction energies (eV) between frontier orbitals within nearest neighbors in crystalline [M(HOEtS-tzdt)$_2$] complexes (M = Ni, Au).

Ni	HO-HO	HO-LU	LU-LU	**Au**	SO-SO
Int **I**	0.1471	0.0366	−0.0592	Int **I**	−0.0913
Int **II**	−0.0929	−0.0432	0.0248	Int **II**	−0.0621
Int **III**	0.0325	−0.0243	0.0250	Int **III**	0.0231

The band structures of both complexes are presented in Fig. 5. As expected from the band filling and the weak intermolecular overlap interactions, the closed-shell nickel complex

Published on 08 April 2020. Downloaded by Bibliotheque de L'Universite de Rennes I on 4/8/2020 12:41:09 PM.

Accepted manuscript

Manuscipt

View Article Online
DOI: 10.1039/D0DT00960A

exhibits a gap between valence (red) and conduction (blue) band. This direct gap is rather large (0.46 eV), and at the origin of its low conductivity. It indicates that in the quest for single-component conductors derived from closed-shell nickel complexes, $[Ni(HOEtS\text{-}tzdt)_2]^0$ is not the best candidate, if we compare it with $[Ni(dmit)_2]^0$ ($\sigma_{RT} = 3.5\times10^{-3}$ S.cm^{-1}),[38,39] or the thiazoline dithiolene derivative $[Ni(Et\text{-}thiazdt)_2]^0$ ($\sigma_{RT} = 1.4\times10^{-2}$ S cm^{-1}).[40]

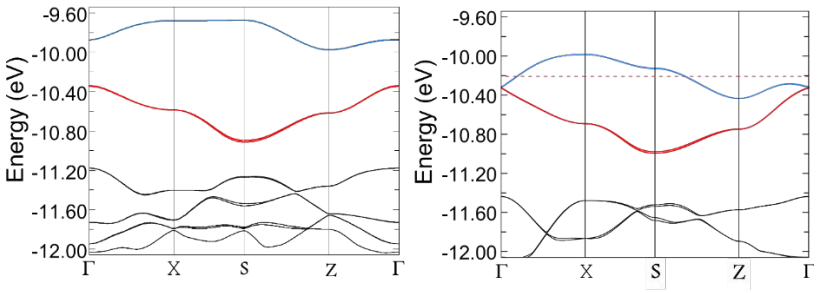

Fig. 5 Calculated band structures for $[Ni(HOEtS\text{-}tzdt)_2]$ (left) and $[Au(HOEtS\text{-}tzdt)_2]$ (right). The HOMO based bands are represented in red and the LUMO ones in blue for the Ni complexes. For the gold complex the SOMO and SOMO-1 based bands are represented in blue and red respectively. The dashed red line represents the Fermi level, assuming a metallic filling of the levels. Γ = (0, 0, 0), X = (1/2, 0, 0), Z = (0, 0, 1/2), M = (1/2, 1/2, 0), S = (1/2, 0, 1/2) of the Brillouin zone of the monoclinic lattice.

On the other hand, thanks to its non-dimerized character, the radical gold complex exhibits a ½-filled SOMO band (in blue) which could lead to a metallic character. The relatively weak dispersion of this band (< 0.5 eV) can explain its observed semiconducting behavior with $\sigma_{RT} = 6\times10^{-2}$ S.cm^{-1} and $E_a = 0.13$ eV (Fig. S6). This compound is thus believed to behave as a Mott insulator, characteristic of such radical systems when they manage to avoid radical dimerization. In that respect, the comparison with the strongly dimerized ethyl-substituted gold complex $[Au(EtS\text{-}tzdt)_2]^{\bullet}$ (See Fig. 3d) is rather enlightening as the latter is a true band semiconductor with σ_{RT}(1 bar) = 3.3×10^{-4} S.cm^{-1}, that is two orders of magnitude below that of $[Au(HOEtS\text{-}tzdt)_2]^{\bullet}$.

Conclusions

We have shown here that the introduction of the hydrogen bond donor group such as the 2-hydroxyethyl one on the 2-alkylthiothiazole-4,5-dithiolate complexes is inducing strong HB interactions with the sp_2 thiazole nitrogen atom, with an enhancement in the neutral complexes relative to the anionic ones. At variance with many other radical gold dithiolene complexes

Published on 08 April 2020. Downloaded by Bibliotheque de L'Universite de Rennes I on 4/8/2020 12:41:09 PM.

Accepted manuscript

Manuscipt

View Article Online
DOI: 10.1039/D0DT00960A

which have a strong tendency to dimerize in the solid state, we have found that $[Au(HOEtS\text{-}tzdt)_2]^{\bullet}$ was crystallizing into uniform stacks, and was isostructural with its neutral, closed-shell nickel analog, another rare situation in this chemistry.[40] It demonstrates how the strength of the HB directing motif can control the overall structural arrangement to stabilize the same structure despite a different electron count. Nevertheless, while the nickel complex behaves as a band semiconductor with weak conductivity (1.6×10^{-5} S.cm^{-1}), the gold complex is described as a Mott insulator with a three orders of magnitude improved conductivity (6×10^{-2} S.cm^{-1}). As such, $[Au(HOEtS\text{-}tzdt)_2]^{\bullet}$ is susceptible to also exhibit an insulator-to-metal transition under pressure[26] or under electric field pulses,[47] as already reported with the thiazoline derivative $[Au(R\text{-}thiazdt)_2]^{\bullet}$ (R = Me, Et). Such investigations will be reported in the near future.

Experimental

General remarks

NMR spectra were recorded at room temperature using $CDCl_3$ unless otherwise noted. Chemical shifts are reported in ppm and ^{1}H NMR spectra were referenced to residual $CHCl_3$ (7.26 ppm) and ^{13}C NMR spectra were referenced to $CHCl_3$ (77.2 ppm). All reagents are commercially available and were used without further purification. Melting points were measured on a Kofler hot-stage apparatus and are uncorrected. Mass spectra were recorded by the Centre Régional de Mesures Physiques de l'Ouest, Rennes and Elemental analysis were at "Service de Microanalyse I.C.S.N.- CNRS 91198" Gif sur Yvette. All the reactions were performed under an argon atmosphere. Methanol, acetonitrile and dichloromethane were dried using inert pure solvent column device. Cyclic voltammetry were carried out on a 10^{-3} M solution of complexes $[Ph_4P][Ni(HOEtS\text{-}tzdt)_2]$ and $[Ph_4P][Au(HOEtS\text{-}tzdt)_2]$ in CH_2Cl_2 with NBu_4PF_6 0.1 M. Voltammograms were recorded at 0.1 Vs^{-1} on a platinum disk electrode. The potentials were measured *versus* Saturated Calomel Electrode (SCE). A Shimatzu 3600 spectrophotometer was employed to record the UV-vis-NIR spectra. The proligand **1** was prepared as previously reported.[41]

Synthesis of 2. Under inert atmosphere, 2-iodoethanol (1 ml, 12.8 mmol) was added to a solution of **1** (200 mg, 0.76 mmol) in 2 mL of DMF. The reaction mixture was stirred at 80°C for 16 hours and then water (200 ml) was added to the medium. The product was extracted with CH_2Cl_2 and the organic phase was washed with water and dried over $MgSO_4$. The solvent was evaporated under vacuum and the crude oil was purified by flash chromatography (eluent: CH_2Cl_2/Petroleum ether; 80:20) giving the compound as a yellow paste in 68 % yield (130 mg,

Published on 08 April 2020. Downloaded by Bibliotheque de L'Universite de Rennes I on 4/8/2020 12:41:09 PM.

Accepted Manuscript

Manuscipt

View Article Online
DOI: 10.1039/D0DT00960A

0.52 mmol); R_f = 0.16 (SiO_2, CH_2Cl_2); ^{1}H NMR (300 MHz) δ 3.97 (t, 2H, OCH_2), 3.43 (t, 2H, SCH_2), 2.52 (s, 1H, OH); ^{13}C NMR (75 MHz, $CDCl_3$) δ 190.3 (C=O), 166.7 (C=N), 142.0 (C=C), 116.5 (C=C), 61.4 (O-CH_2), 38.0 (S-CH_2); HRMS (ESI) $[M+Na]^+$ Calcd for $C_6H_5NNaO_2S_4$: 273.9095; Found: 273.9097.

Synthesis of monoanionic complexes [PPh_4][Ni(HOEtS-tzdt)$_2$] and [PPh_4][Au(HOEtS-tzdt)$_2$]. To dry MeOH (10 ml) under inert atmosphere, sodium metal (146 mg, 6.36 mmol) was added. The methanolate solution was then transferred to the protected ligand **2** (200 mg, 0.79 mmol). After complete dissolution the solution was stirred for 30 min at room temperature. Then a solution of $NiCl_2.6H_2O$ (95 mg, 0.4 mmol), or $KAuCl_4$, (151 mg, 0.4 mmol) in pure water (10 mL) was added, followed 6 hours later by the addition of Ph_4PBr (**Ni:** 370 mg, 0.88 mmol; **Au:** 185mg, 0.44 mmol). After stirring for 15 h, the formed precipitate was filtered and recrystallized from CH_2Cl_2/MeOH 20/80 to afford the monoanionic complex [PPh_4][Ni(HOEtS-tzdt)$_2$] as dark blue crystals, and from warm CH_3CN to afford [PPh_4][Au(HOEtS-tzdt)$_2$] as purple crystals.

[PPh_4][Ni(HOEtS-tzdt)$_2$]: $C_{34}H_{30}N_2NiO_2PS_8$. Yield: 41% (140 mg, 0.33 mmol)); mp = 182°C; HRMS (ESI) [Ni(HOEtS-tzdt)$_2$]$^-$ calcd for $C_{10}H_{10}N_2NiO_2S_8$: 503.7867. Found: 503.7862; Anal. Calcd. for $C_{34}H_{40}N_2NiO_2PS_8$: C, 48.34; H, 3.58; N, 3.32. Found: C, 48.30; H, 3.51; N, 3.21.

[PPh_4][Au(HOEtS-tzdt)$_2$]: $C_{34}H_{30}N_2AuO_2PS_8$. Yield: 37% (125 mg, 0.25 mmol)); mp = 176°C; ^{1}H NMR (300 MHz, DMSO-d6) δ 8.00-7.93(m, 4H, Ar), 7.85-7.70 (m, 16H, Ar), 5.01 (t, 2H, J = 6 Hz, OH), 3.63 (q, 4H, J = 6 Hz, OCH_2), 3.14 (t, 4H, J = 6 Hz, SCH_2); HRMS (ESI) [Au(HOEtS-tzdt)$_2$]$^-$ calcd for $C_{10}H_{10}N_2AuO_2S_8$: 642.8179 Found: 642.8182; Anal. Calcd. for $C_{34}H_{40}N_2AuO_2PS_8$: C, 41.54; H, 3.08; N, 2.85. Found: C, 41.51; H, 2.78; N, 2.76.

Electrocrystallizations

They were performed in two-compartment cells with Pt electrodes (length 1cm, diameter 1 mm). [Ni(HOEtS-tzdt)$_2$]^0 was obtained from the electrocrystallization of [Ph_4P][Ni(HOEtS-tzdt)$_2$] (10 mg) in 12 mL of CH_3CN/CH_2Cl_2 (2/1) at room temperature in the presence of NBu_4PF_6 (200 mg) as supporting electrolyte with a current of 0.2 μA. [Au(HOEtS-tzdt)$_2$]$^\bullet$ was obtained from the electrocrystallization of [Ph_4P][Au(HOEtS-tzdt)$_2$] (10 mg) in 12 mL of CH_3CN/CH_2Cl_2 (7/3) at RT in the presence of NBu_4PF_6 as supporting electrolyte with a current of 0.5 μA. Black crystals were harvested on the anode after 7 days.

Published on 08 April 2020. Downloaded by Bibliotheque de L'Universite de Rennes I on 4/8/2020 12:41:09 PM.

Accepted Manuscript

View Article Online
DOI: 10.1039/D0DT00960A

Published on 08 April 2020. Downloaded by Bibliotheque de L'Universite de Rennes I on 4/8/2020 12:41:09 PM.

Resistivity measurements

The resistivity measurements at ambient pressure were performed in four points for the Au complex (but only in two-point for the Ni complex with much smaller crystals), along the long axis of the needles using a DC current in the range of I_{dc}= 0.1−1 μA, and gold wires (10 μm in diameter) were attached to with carbon paste.

Band structure calculations

The tight-binding band structure calculations and $\beta_{HOMO/LUMO}$ interaction energies were based upon the effective one-electron Hamiltonian of the extended Hückel method,[48] as implemented in the Caesar 2.0 chain of programs.[49] The off-diagonal matrix elements of the Hamiltonian were calculated according to the modified Wolfsberg−Helmholz formula.[50] All valence electrons were explicitly taken into account in the calculations and the basis set consisted of double-ζ Slater-type orbitals for the metal and chalcogen atoms, and single-ζ Slater-type orbitals for the rest of the atoms. The exponents, contraction coefficients, and atomic parameters are detailed in supplementary material.

X-Ray Crystallography

Details of the structural analyses for the three compounds are summarized in Table 5. Data collections were performed on an APEXII Bruker-AXS diffractometer equipped with a CCD camera for $[Ni(HOEtS\text{-}tzdt)_2]^0$, and on D8 VENTURE Bruker AXS diffractometer for $[Ph_4P][Au(HOEtS\text{-}tzdt)_2]$, and $[Au(HOEtS\text{-}tzdt)_2]^{\bullet}$. Structures were solved by direct methods using the *SHELXT* program, then refined with full-matrix least-square methods based on F^2 (*SHELXL-2014*).[51] All non-hydrogen atoms were refined with anisotropic atomic displacement parameters. Except oxygen-linked hydrogen atoms that were introduced in the structural model through Fourier difference maps analysis, H atoms were finally included in their calculated positions. Disorder on one hydroxyethyl moiety in one of the three crystallographically independent anionic gold complex (on Au2) in $[Ph_4P][Au(HOEtS\text{-}tzdt)_2]$ was refined with a 62:38 distribution.

Accepted manuscript

Manuscipt

View Article Online
DOI: 10.1039/D0DT00960A

Published on 08 April 2020. Downloaded by Bibliotheque de L'Universite de Rennes I on 4/8/2020 12:41:09 PM.

Table 5 Crystallographic data

Compound	$[Ph_4P]$ $[Au(HOEtS\text{-}tzdt)_2]$	$[Ni(HOEtS\text{-}tzdt)_2]$	$[Au(HOEtS\text{-}tzdt)_2]$
CCDC	1989998	1989996	1989997
Formula	$C_{34}H_{30}AuN_2O_2PS_8$	$C_{10}H_{10}NiN_2O_2S_8$	$C_{10}H_{10}AuN_2O_2S_8$
FW (g.mol^{-1})	983.01	505.38	643.65
Crystal system	monoclinic	monoclinic	monoclinic
Space group	$P2_1/c$	$P2_1/n$	$P2_1/n$
a (Å)	26.407(2)	5.0235(3)	4.9715(6)
b (Å)	18.2569(15)	27.1171(19)	27.272(3)
c (Å)	23.1623(19)	6.1914(4)	6.1720(8)
α (°)	90	90	90
β (°)	98.355(3)	92.475(2)	91.722(5)
γ (°)	90	90	90
V (Å^3)	11048.2(15)	842.62(9)	836.43(17)
T (K)	150(2)	296(2)	150(2)
Z	12	4	2
D_{calc} (g·cm^{-3})	1.757	1.992	2.556
μ (mm^{-1})	0.796	2.148	9.799
Total refls.	115068	4281	9054
Uniq. refls. (R_{int})	25275(0.0688)	1920 (0.0351)	1914 (0.0397)
Unique refls. (I>2s(I))	16178	1523	1766
R_1, wR_2	0.0670, 0.1500	0.0395, 0.0888	0.0499, 0.0978
R_1, wR_2 (all data)	0.1269, 0.1931	0.0563, 0.0940	0.0560, 0.0993
GoF	1.063	1.037	1.468

Conflicts of interest

There are no conflicts to declare.

Acknowledgements

Accepted manuscript

Manuscipt

View Article Online
DOI: 10.1039/D0DT00960A

Support of University Rennes 1 for a PhD grant (to H. H.) is acknowledged. We thank Z. Xu for preliminary synthesis experiments, Th. Roisnel, V. Dorcet and O. Jeannin (ISCR, Rennes) for the X-ray crystal structure resolutions and Th. Guizouarn for the SQUID measurements.

Notes and references

1 Dithiolene Chemistry, *Prog. Inorg. Chem*., E. I. Stiefel Ed. 2004, vol. 52.

2 P. Cassoux, L. Valade, H. Kobayashi, A. Kobayashi, R. A. Clark and A. E. Underhill, *Coord. Chem. Rev.*, 1991, **110**, 115−160.

3 R.-M. Olk, B. Olk, W. Dietzsch, R. Kirmse and E. Hoyer, *Coord. Chem. Rev.*, 1992, **117**, 99−131.

4 P. Cassoux, *Coord. Chem. Rev.*, 1999, **185−186**, 213-232.

5 A. E. Pullen and R.-M. Olk, *Coord. Chem. Rev.*, 1999, **188**, 211−262.

6 N. Robertson and L. Cronin, *Coord. Chem. Rev.*, 2002, **227**, 93−127.

7 M. L. Mercuri, P. Deplano, L. Pilia, A. Serpe and F. Artizzu, *Coord. Chem. Rev.*, 2010, **254**, 1419−1433.

8 F. Pop and N. Avarvari, *Coord. Chem. Rev.*, 2017, **346**, 20−31.

9 T. Kusamoto and H. Nishihara, *Coord. Chem. Rev.*, 2019, **380**, 419−439.

10 R. Kato, *Bull. Chem. Soc. Jpn*., 2014, **87**, 355−374.

11 R. Kato, *Chem. Rev.,* 2004, **104**, 5319−5346.

12 N. C. Schiødt, T. Bjørnholm, K. Bechgaard, J. J. Neumeier, C. Allgeier, C. S. Jacobsen and N. Thorup, *Phys. Rev. B*, 1996, **53**, 1773−1778.

13 D. Belo, H. Alves, E. B. Lopes, M. T. Duarte, V. Gama, R. T. Henriques, M. Almeida, A. Pérez-Benítez, C. Rovira and J. Veciana, *Chem. Eur. J.,* 2001, **7**, 511−519.

14 O. J. Dautel, M. Fourmigué, E. Canadell and P. Auban-Senzier, *Adv. Funct. Mater.*, 2002, **12**, 693−698.

15 T. Higashino, O. Jeannin, T. Kawamoto, D. Lorcy, T. Mori and M. Fourmigué, *Inorg. Chem*. **2015**, *54*, 9908−9913.

16 D. G. Branzea, F. Pop, P. Auban-Senzier, R. Clérac, P. Alemany, E. Canadell and N. Avarvari, *J. Am. Chem. Soc*., 2016, **138**, 6838–6851.

17 M. M. Andrade, R. A. L. Silva, I. C. Santos, E. B. Lopes, A. Rabaça, L. C. J. Pereira, J. T. Countinho, J. P. Telo, C. Rovira, M. Almeida and D. Belo, *Inorg. Chem. Front.*, 2017, **4**, 270-280.

Published on 08 April 2020. Downloaded by Bibliotheque de L'Universite de Rennes I on 4/8/2020 12:41:09 PM.

Accepted manuscript

Manuscipt

View Article Online
DOI: 10.1039/D0DT00960A

Published on 08 April 2020. Downloaded by Bibliotheque de L'Universite de Rennes I on 4/8/2020 12:41:09 PM.

18 S. A. Baudron, N. Avarvari and P. Batail, *Inorg. Chem*., 2005, **44**, 3380-3382.

19 S. Debnath, H. S. Srour, B. Donnio, M. Fourmigué and F. Camerel, *RSC Adv*., 2012, **2**, 4453–4462.

20 F. Camerel and M. Fourmigué, *Eur. J. Inorg. Chem.,* 2020, 508–522.

21 T. Bsaibess, M. Guerro, Y. Le Gal, D. Sarraf, N. Bellec, M. Fourmigué, F. Barrière, V. Dorcet, T. Guizouarn, T. Roisnel and D. Lorcy, *Inorg. Chem*., 2013, **52**, 2162−2173.

22 Y. Le Gal, T. Roisnel, P. Auban-Senzier, T. Guizouarn and D. Lorcy, *Inorg. Chem*., 2014, **53**, 8755−8761.

23 S. Yokomori, A. Ueda, T. Higashino, R. Kumai, Y. Murakami and H. Mori, *CrystEngComm*., 2019, **21**, 2940−2948.

24 (*a*) M. Fourmigué and P. Batail, *Chem. Rev*., 2004, **104**, 5379−5418. (b) N. Mroweh, F. Pop, C. Mézière, M. Allain, P. Auban-Senzier, N. Vanthuyne, P. Alemany, E. Canadell, and N. Avarvari, *Cryst. Growth Des*., 2020, **20**, 4, 2516−2526 and references therein..

25 S. Eid, M. Fourmigué, T. Roisnel and D. Lorcy, *Inorg. Chem*., 2007, **46**, 10647-10654.

26 N. Tenn, B. Bellec, O.Jeannin, L. Piekara-Sady, P. Auban-Senzier, J. Íñiguez, E. Canadell and D. Lorcy, *J. Am. Chem. Soc*., 2009, **131**, 16961–16967.

27 G. Yzambart, N. Bellec, G. Nasser, O. Jeannin, T. Roisnel, M. Fourmigué, P. Auban-Senzier, J. Íñiguez, E. Canadell and D. Lorcy, *J. Am. Chem. Soc*., 2012, **134**, 17138–17148

28 A. Filatre-Furcate, T. Roisnel, M. Fourmigué, O. Jeannin, N. Bellec, P. Auban-Senzier and D. Lorcy, *Chem. Eur. J.*, 2017, **23**, 16004–16013

29 A. Filatre-Furcate, N. Bellec, O. Jeannin, P. Auban-Senzier, M. Fourmigué, J. Íñiguez, E. Canadell, B. Brière, V. Ta-Phuoc and D. Lorcy, *Inorg. Chem.*, 2016, **55**, 6036–6046

30 Y. Le Gal, T. Roisnel, P. Auban-Senzier, N. Bellec, J. Íñiguez, E. Canadell and D. Lorcy, *J. Am. Chem. Soc.*, 2018, **140**, 6998–7004.

31 B. Garreau-de Bonneval, K. I. Moineau-Chane Ching, F. Alary, T.-T. Bui and L. Valade, *Coord. Chem. Rev*., 2010, **254**, 1457−1467.

32 A. Kobayashi, E. Fujiwara and H. Kobayashi, *Chem. Rev.,* 2004, **104**, 5243−5264.

33 A. Kobayashi, H. Tanaka, M. Kumasaki, H. Torii, B. Narymbetov and T. Adachi, *J. Am. Chem. Soc.,* 1999, **121**, 10763–10771.

34 H. Tanaka, Y. Okano, H. Kobayashi, W. Suzuki and A. Kobayashi, *Science,* 2001, **291**, 285−287.

Accepted manuscript

Manuscipt

View Article Online
DOI: 10.1039/D0DT00960A

Published on 08 April 2020. Downloaded by Bibliotheque de L'Universite de Rennes I on 4/8/2020 12:41:09 PM.

35 H. Cui, J. S. Brooks, A. Kobayashi and H. Kobayashi, *J. Am. Chem. Soc.*, 2009, **131**, 6358–6359.

36 H. Cui, H. Kobayashi, S. Ishibashi, M. Sasa, F. Iwase, R. Kato and A. Kobayashi, *J. Am. Chem. Soc.*, 2014, **136**, 7619–7622.

37 J. P. M. Nunes, M. J. Figueira, D. Belo, I. C. Santos, B. Ribeiro, E. B. Lopes, R. T. Henriques, J. Vidal-Gancedo, J. Veciana, C. Rovira and M. Almeida, *Chem. Eur. J.*, 2007, **13**, 9841 – 9849.

38 L. Valade, J.-P. Legros, M. Bousseau, P. Cassoux, M. Garbauskas and L. V. Interrante, *J. Chem. Soc. Dalton Trans.,* 1985, 783−794.

39 H. B. Cui, T. Tsumuraya, T. Miyazaki, Y. Okano and R. Kato, *Eur. J. Inorg. Chem.*, 2014, **24**, 3837–3840.

40 A. Filatre-Furcate, N. Bellec, O. Jeannin, P. Auban-Senzier, M. Fourmigué, A. Vacher and D. Lorcy, *Inorg. Chem.*, 2014, **53**, 8681–8690.

41 (*a*) A. Filatre-Furcate, P. Auban-Senzier, M. Fourmigué, T. Roisnel, V. Dorcet and D. Lorcy, *Dalton Trans.,* 2015, **44**, 15683–15689; (*b*) A. Filatre-Furcate, T. Roisnel and D. Lorcy, *J. Organomet. Chem.*, 2016, **819**, 182–188.

42 H. Hachem, Z. Xu, N. Bellec, O. Jeannin, P. Auban-Senzier, T. Guizouarn, M. Fourmigué and D. Lorcy, *Dalton Trans.,* 2018, **47**, 6580–6589.

43 G. A. Jeffrey, *An introduction to Hydrogen Bonding*, Oxford University Press, Oxford, 1997.

44 T. Steiner, *Angew. Chem. Int. Ed*., 2002, **41**, 48−76.

45 R. Kirmse, M. Kampf, R.-M. Olk, M. Hildebrand and H. Krautscheid, *Z. Anorg. Allg. Chem*., 2004, **630**, 1433−1436.

46 V. Hernandez, C. Castiglioni, M. Del Zoppo and G. Zerbi, *Phys. Rev. B*, 1994, **50**, 9815−9823.

47 (*a*) P. Stoliar, P. Diener, J. Tranchant, B. Corraze, B. Brière, V. Ta-Phuoc, N. Bellec, M. Fourmigué, D. Lorcy, E. Janod and L. Cario. *J. Phys. Chem. C.*, 2015, **119**, 2983−2988 ; (*b*) C. Adda, B. Corraze, P. Stoliar, P. Diener, J. Tranchant, A. Filatre-Furcate, M. Fourmigué, D. Lorcy, M.-P. Besland, E. Janod and L. Cario. *J. Appl. Phys.*, 2018, **124**, 152124 (1-7).

48 M.-H. Whangbo and R. Hoffmann, *J. Am. Chem. Soc.,* 1978, **100**, 6093−6098.

Accepted manuscript

Manuscipt

View Article Online
DOI: 10.1039/D0DT00960A

49 J. Ren, W. Liang and M.-H. Whangbo, Crystal and Electronic Structure Analysis Using CAESAR; PrimeColor Software, Inc.: Cary, NC, 1998.

50 J. Ammeter, H.-B. Burgi, J. Thibeault and R. Hoffmann, *J. Am. Chem. Soc.*, 1978, **100**, 3686−3692.

51 G. M. Sheldrick, *Programs for the Refinement of Crystal Structures*; University of Göttingen: Göttingen, Germany, 1996.

Published on 08 April 2020. Downloaded by Bibliotheque de L'Universite de Rennes I on 4/8/2020 12:41:09 PM.

Accepted manuscript

Manuscipt

View Article Online
DOI: 10.1039/D0DT00960A

For Table of content

Nickel (closed-shell) or gold (radical) bis(dithiolene) neutral complexes, functionalized with hydroxyethyl and thiazole moieties, afford hydrogen-bonded single component conductors.

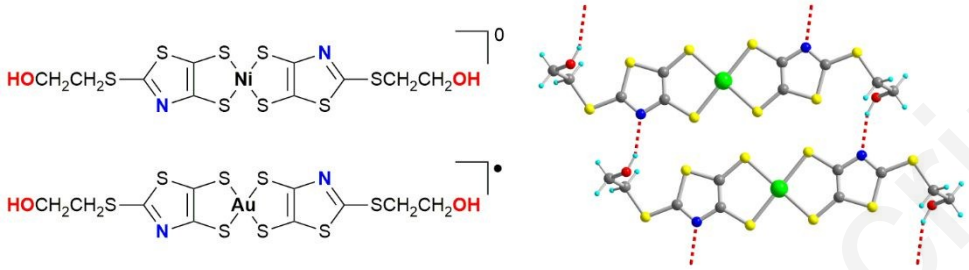

Published on 08 April 2020. Downloaded by Bibliotheque de L'Universite de Rennes I on 4/8/2020 12:41:09 PM.

Accepted manuscript

Manuscipt